Forecasting Research

Forecasting Research Division
Technical Report No. 65

An Investigation Into The Sensitivity Of A Viscous-Plastic Sea Ice Model To UM Analysed Winds

by
C G Sherlock

August 1993

Meteorological Office
London Road
Bracknell
Berkshire
RG12 2SZ
United Kingdom

Forecasting Research Division
Technical Report No. 65

An Investigation Into The Sensitivity Of A Viscous-Plastic Sea Ice Model To UM Analysed Winds

by

C G Sherlock

August 1993

Forecasting Research Division
Meteorological Office
London Road
Bracknell
Berkshire RG12 2SZ
ENGLAND

N.B. This paper has not been published. Permission to quote from it must be obtained from the above Met. Office division.

Abstract

A dynamic-thermodynamic sea ice model, based on that of Hibler (1979), is investigated for its sensitivity to Numerical Weather Prediction wind forcing. Three parallel integrations are performed using winds derived from the 1992 Unified Model geopotential analyses of heights at 1000mb and 850mb, and pressure at mean sea level (pmsl); other forcing fields are the same for all three runs. The model takes about two years to spin-up. Winds derived from the 1000mb height and pmsl are very similar and model results from the runs are almost identical. The low level winds and those derived from 850mb show a similar overall circulation; the differences between them produce changes to the model ice drift of roughly the same relative magnitude. Instantaneous model ice thicknesses taken from January, April, July, and October show similar overall patterns, and differ by less than 1m for most of the grid over most of the integration. Model ice circulation and thickness distribution are consistent with those obtained by Walsh et al. (1985) in a 30 year run of a similar model. However, the predicted position of the ice edge compares poorly with satellite data from 1992.

1. Introduction

The Forecasting Ocean Atmosphere Model (FOAM) is planned to form the basis of an ocean forecast system, with the Royal Navy as primary customer. FOAM will be driven by fluxes of heat, momentum, and fresh water obtained from the Meteorological Office's Numerical Weather Prediction (NWP) model. One of the requirements for FOAM is to predict ice edge, ice concentration and thickness, and ice drift on the sea surface, in and around the polar regions - both as an end, and as a means of producing better forecasts of other ocean parameters. Variables such as ocean temperature, salinity, and stability, can be changed by the production, persistence, or melting of sea ice.

A numerical model of sea ice has been picked for incorporation into FOAM. The model (Hibler, 1979; Hibler, 1980; Hibler and Walsh, 1982; Hibler and Bryan, 1987) has proved itself suitably accurate in predicting ice build up, decay, and motion, and is already part of the US Polar Ice Prediction System (PIPS) which has been running operationally for several years (Preller and Posey, 1989 ; Riedlinger and Preller, 1991).

The FOAM group has an experimental version of the ice-model, dating from around 1986. This version runs on a square grid, which covers all of the Arctic Ocean, and the Fram Strait (which leads to the North Atlantic) as far south as mid Scandinavia. The resolution of the land mask and the daily forcing data which were supplied with the model is 223.6 km; the origin of the forcing data is unknown. The model is set up to run for a 360 day year with a time step of one day, and produces monthly output fields of ice velocity, effective ice thickness (the thickness the ice would have if it were spread evenly across the whole grid square), and ice concentration (the fraction of the grid square covered by ice). The following forcing fields are required: geostrophic atmospheric winds, geostrophic ocean currents, heat flux from the deep ocean, air temperature, air humidity, total incoming short wave radiation, and total incoming longwave radiation.

This study was designed to investigate the response of the ice model to wind forcing from the Unified Model (UM) analysed winds. In its current form, the ice-model takes geostrophic wind velocities as part of its dynamic forcing; three parallel runs of the model were made, with daily varying winds derived from the 1992 Met. Office WGDOS archives of 1000mb height, 850mb height, and the pressure at mean sea level (pmsl), using the same thermodynamic forcing data. It was hoped that these runs would allow the internal

consistency of the NWP fields to be assessed, as well as achieving the main aim of validating the response of the ice model.

This report details the derivation of the winds and their interpolation onto the model grid. The results are examined for consistency, and compared with those of Walsh et al. (1985), who ran a similar model with 30 years of archived forcing; they are also compared with the several satellite observations of ice edge during 1992, derived from the weekly U.S. Joint Ice Centre (JIC) bulletins. There is a brief investigation of the model spin-up.

2. The Forcing Winds

The main aim of the experiment was to assess the sensitivity of the model to three different measures of the same atmospheric winds. However, the model runs can also be considered as a control and two perturbation experiments and the model examined for sensitivity to the sizes of the perturbations. The method for calculating the geostrophic winds is described in the appendix. A brief comparison between annual means of the three sets of forcing data (fig. 1) now follows.

A single, constant air density (independent of pressure, temperature, and humidity) was used in the calculation of geostrophic winds from pmsl; variations on the chosen value of around $\pm 10\%$ might be expected in reality. As they are at roughly the same level, we would expect pmsl and 1000mb winds to be very similar if the true air densities were used; the choice of a constant air density has not produced inaccuracies large enough to be visible in the charts of fig. 1. Slight discrepancies between annual mean winds from the 1000mb heights and those from pmsl are visible in contour maps of the wind magnitudes (not shown).

The general circulation is roughly the same in all three charts, with large scale patterns of high and low wind speed reproduced in similar areas (though not necessarily with the same magnitudes). Above the sea, the overall pattern appears to be stronger and clearer at 850mb than at 1000mb or mean sea level. There is a significant discrepancy in wind direction east of Scandinavia, with southerly and then easterly winds on the low level charts and strong westerlies at 850mb, suggesting a detailed boundary layer structure.

The winds derived from lower levels tend to be more patchy than those at 850mb, showing a much larger small scale variability in magnitude and direction. Several regions of high wind speed are visible over the Canadian Archipelago and just east of Greenland, whilst the Beaufort and Chukchi seas are subject to relatively slow and uncertain wind forcing. The low level winds show a small but definite clockwise gyre in the Beaufort sea, a phenomenon that the annual mean of the more forceful 850mb winds lacks.

3. Results

The viscous-plastic ice model calculates a wind stress which acts at a pre-specified 'turning' angle to the geostrophic wind with a magnitude proportional to the square of the wind speed. The model was run for three years for each of the three forcings, at which time (see 3C) the ice was considered to have settled into an annually repeating pattern. The first part of this section compares the model results for year three of each run; there follows a comparison with satellite derived ice edge data from 1992, and with the 30 year run of Walsh et al. (1985). Finally there is a brief investigation of the model spin-up. Shading of the ice depth charts is dotted between the two and three metre contours and lined between the depth contours of four and five metres.

A. Intercomparison Of The Three Runs

The months of January, April, July, and October are examined as samples of the seasons in which they occur. Velocity fields are monthly means, ice depth and concentration are instantaneous values from the end of the month. Annual mean ice velocities are also examined. The charts of ice concentration will not be shown as they offer very little information for comparison; with a few exceptions the model shows ice cover of either zero or in excess of 80%, so that for the most part, the ice edge is given fairly accurately by the drop of ice thickness to zero.

Annual Mean Velocity Fields

The annual mean velocity fields (fig. 2) all show a transpolar drift, and a very similar overall circulation. As hoped and expected, the charts resulting from pmsl and 1000mb forcing are almost identical, and hence the model sensitivity to winds is not extreme.

All three show an anticyclonic gyre in the Beaufort sea, but it is much less pronounced, and the ice moves more slowly, when subjected to the 850mb forcing. Physically, the ice is driven by surface winds and so one would expect the model circulations caused by the lower level winds to be more representative.

From northern Greenland, across the Fram Strait to western Scandinavia, the three fields are very similar. The slightly faster ice movement off the coast of Norway, and slower off the coast of Greenland, with 850mb forcing correspond to slightly stronger and lighter

winds at that level respectively.

The most significant difference in circulation occurs in the Barents Sea (east of Spitsbergen, north of Scandinavia) with a basically westerly motion caused by the 850mb winds, and a southerly then easterly drift in the other two runs. A minor discrepancy between the charts from low and high level forcing, associated with the Beaufort Gyre, consists of a complete reversal in drift direction off the coast of eastern Alaska. The westward drift caused by the low level winds is closer to the model climatologies of Walsh et al. (1985) (e.g. figs 10e and 10f).

January

The charts for January (figs 3a, 4a, 5a, 6a, 7a, and 8a) show the 3m thickness contour extending much further towards the Eurasian coast when the 850mb winds are applied although the 2m contours are in much the same places on all three charts. The 1000mb and pmsl ice is up to a metre thicker than the 850mb both to the north and east of Greenland, although the ice edge east of Greenland is in the same position for all three forcings. A strong Beaufort Gyre is present in all three velocity fields, although it is further south in the 850mb chart. The transpolar drift appears to have been twisted by all three winds so that it heads from the middle of the Eurasian coast, straight across the pole to the north coast of Greenland.

April

All three April velocity charts (figs 3b, 4b, and 5b) find the ice moving in a direction contrary to the accepted transpolar drift, most strongly in the 850mb chart. Support for these model predictions is found in April pmsl anomalies (1983 to 1992) given by the Weather Log (1983-1992), which suggest a major shift (from the norm) in the cross-polar wind direction of April 1992. For eight of the twelve Aprils examined the wind direction across the pole is from the Bering Strait to Greenland, which corresponds to the usual transpolar ice drift direction; in both April 1984 and April 1989 there are high pressure anomalies centred close to the pole, suggesting very light winds in that area. Only two of the charts (1987 and 1992) show a reversal of the preferred wind direction, with flow from the Fram Strait to the Bering Strait; it is likely that the modelled ice drift reversals result from this.

The 'Beaufort Gyres' of the pmsl and the 1000mb runs are translated significantly

northwestwards of their usual position, and in the 850mb run the full circle of the gyre is not quite completed. The predicted drift directions are very similar over the whole of the model grid, although frequent variations in magnitude occur. As in January, the 3.0m depth contour is a little closer to Siberia with 850mb winds than with the lower level forcing (figs 6b, 7b, and 8b); the ice is thicker everywhere in the 850mb chart except to the northeast of Greenland and in the 'Beaufort Gyre'. The latter is possibly a convergence effect, similar to that produced by anticyclonic gyres in open water.

July

The July velocity charts (figs 3c, 4c, and 5c) all show the Beaufort Gyre to be elongated parallel to the Alaskan coast. The 850mb winds again produce a less pronounced gyre, further south than that of the lower winds. Again there is no transpolar drift, but a cyclonic polar gyre appears in all three charts. There are a few other small differences between the circulations caused by low and high level winds, most notably in the East Greenland Sea where the ice driven by 1000mb and pmsl winds is much more variable in direction. Thickness distributions (figs 6c, 7c, and 8c) are very similar, although the 850mb ice is up to a metre thicker than the other two fields off the north coasts of Greenland and Canada. All three ice fields have a low ice concentration (< 0.5) to the north of Siberia as is usual for this time of year (not shown).

October

All three October drift charts (figs 3d, 4d, and 5d) show a full transpolar drift, running strongly from the Siberian coast, right through to the Fram Strait. In this month, the Beaufort gyre is only truly present in ice driven by 850mb winds, as the circulation is incomplete in the lower level charts. The 850mb winds also produce two additional (minor) gyres in the Beaufort and Chukchi seas, only the ghosts of which are present in the 1000mb and pmsl charts. The thickness fields (figs 6d, 7d, and 8d) are also fairly close; the 3m contour may extend further towards the Eurasian coast with 850mb winds (as in the two of the three previous examples) but all show a significant retreat of the ice edge up the Fram Strait (although the 850mb edge retreats a little further than the other two) and by the Bering Strait and eastern Siberia.

B. Comparison With Other Data

The three sets of model ice fields (from 1000mb, 850mb, and pmsl) were fairly similar and so those fields obtained from winds at 1000mb will be taken as representative for comparison with other data.

Four ice fields were reconstructed from the *JIC ice edge* bulletins of 1992 (fig. 9a-d); validity dates were January 17th, April 10th, June 12th, and October 16th. No bulletins were received during July of 1992 and so the closest bulletin was taken. Model results are taken from the ends of January, April, June, and October (figs 9e-h) - so differences between corresponding fields would be expected even if the model made perfect predictions. As it is, only the wind forcing for the model is from 1992, the source of the remaining fluxes is unknown (but it cannot be from 1992 as it was received before 1991) so that there are many reasons to expect a poor simulation by the model.

January

In January the model produces too much ice in the Fram Strait. Southern and western Spitsbergen are ice free, according to the satellite data, but the island is surrounded by ice at least half a metre thick in the model. This ice is fairly thin and might be thought to cover little of the sea-surface, but each model grid square shows a compactness (fractional ice cover) in excess of 0. 8 (not shown), so the observed open water is not even approximated by the model.

April

In April, the model predicts the ice off Greenland and west and south of Spitsbergen fairly well, but again fails to produce the open water in the Barents Sea north of Scandinavia. However the cover is less compact than in January (model ice concentrations lie between 0.2 and 0.8 over most of the Barents Sea).

June

For both of the above months, ice was modelled and observed over the whole of the Pacific/Alaskan/Siberian side of the Arctic. A significant retreat of the ice is predicted between April and June, in the Chukchi, Greenland, and Barents seas. Satellite data show that the open water of the Barents Sea has extended further north by June - though the east

coast of Spitsbergen is not ice free (as the model predicts). The observed ice edge east of Greenland shows no noticeable change from its position in April, and the Chukchi Sea also remains covered in ice.

October

October satellite data show a small ice edge retreat near the Bering Strait which is exaggerated and premature (it was evident in June) in the model, but is nonetheless present. The modelled and observed edge in and just east of the Barents Sea are much the same - the model has (perhaps for the wrong reasons) caught up with reality. Similarly, Spitsbergen is virtually ice free in both prediction and observation. There is still a significant discrepancy east of Greenland with ice observed almost as far south as Iceland, and the modelled edge over a thousand kilometres to the north.

It is fair to say that, excepting the east coast of Greenland, the model is overpredicting ice in winter and spring and underpredicting it in summer and autumn - it is too extreme. The poor quality results in the Greenland Sea are an accepted characteristic of the Hibler model when run on its own. The accuracy is improved dramatically when the ice model is coupled with a model of the ocean (Hibler and Bryan, 1987) which is able to supply much more realistic heat fluxes. Premature summer melt is another well known problem with the model as it does not allow for the retarding effects of snow cover and heat storage within the ice.

Walsh et al. (1985) ran a version of the Hibler ice model using forcing derived from archived data for 1951-1980. The major difference between their model and that run at the Met. Office involves the discretisation of temperature within the ice. The version at the Met. Office uses 'slab thermodynamics' where the model has a linear internal temperature profile, determined by the temperatures at the top and bottom of the ice. Walsh et al. (1985) divide the ice into seven thermodynamic layers with a temperature and heat flux calculated at each one. The idea is to allow the ice base and interior to respond more slowly and more naturally to atmospheric changes.

In their 1985 paper, Walsh et al. show 30 year means of February and August ice thicknesses (figs 10a-b). These show a similar pattern to ice thicknesses obtained using 1992

winds at 1000mb (figs 6e-f), but the 1992 ice is roughly a third again as thick as the 30 year mean. It is not known how much of this is the result of the altered thermodynamics, and how much is just natural variation from a long term mean. August extents in the Greenland sea are very similar, but Walsh et al. find on average, more ice there during February than given by the 1992 run.

Modelled ice extents (and thicknesses) for August 1968 and August 1975 (figs 10c and 10d) from Walsh et al. (1985) show the 30 year summer extremes of ice edge in the Alaska/eastern Siberia area; our 1992 predictions fall between the two of them.

Thirty year seasonal and annual mean velocity fields are also given by Walsh et al. (1985) (not shown). These resemble model output for the most part only in general trends, and there are sometimes sizeable differences between the magnitudes and extents of our results and those of Walsh et al. (1985). For example our April 1992 output shows a reversal of the transpolar gyre which is not present in Walsh's 30 year mean for April, although, as we have seen, it is consistent with Weather Log data. Walsh et al themselves compare two five year mean velocity fields (1951-55 and 1976-80, figs 10e and 10f). These only resemble each other in general terms - for instance: both have a transpolar drift and southwards flowing current to the east of Greenland (although the magnitudes of the currents differ) and the latter has a much more pronounced Beaufort Gyre and - so the differences between the 1992 results and those of Walsh et al. fall easily within the bounds of natural variability.

C. The Model Spin-up

For similar reasons to those cited in the previous section, only the results from the 1000mb run will be examined here.

The model starts off with an initial ice thickness field of 2.2m everywhere except in the Fram Strait at the edge of the grid (where the thickness is set to zero). At the end of the first month (fig. 11a) the ice has already become thicker/thinner by up to a metre depending upon position. Excess ice in the Fram Strait has started to melt and there is a build up off the north coasts of Greenland and Canada. By April (11b), the pattern resembles that expected of the ice thickness - although there are still several differences between it and the April of the following year's cycle. Similarly for June and October (figs 11c and 11d). There are no noticeable differences corresponding charts for years two and three - seasonal equilibrium has been achieved.

Velocity spins up to seasonal equilibrium very quickly indeed (fig. 12) - between the January mean of year one and that of year two there are only minor differences; and April shows little difference between the years. Slight discrepancies are still apparent in charts of ice drift speed (not shown) between October of years one and two, but are far from obvious when the arrow representation is used. Differences of this order (i.e. a few grid squares out by 0.03 ms^{-1}) persist between years two and three of the run.

4. Conclusions

1. The model is not overly sensitive to the type of UM forcing - geostrophic winds from pmsl and 1000mb height are almost identical and so are the resulting ice drifts and build-ups. Noticeable differences in the modelled ice circulations and thickness distributions arise when the model is forced by winds from the 850mb height instead of the low level winds, but the model results are, for the most part, fairly similar.

2. The model produces just a circulation and thickness distribution when driven by winds derived from UM output which are well within the bounds of model variability found by Walsh et al. (1985).

3. It was always possible that geostrophic winds could have been by far the most dominant forcing term for the model, so that, if the model were good enough, accurate predictions of 1992 ice extent would have been made. The results are in fact no closer to the observations than the 30 year monthly extents of Walsh, which can be taken as a climatology of the model. Hence more than just geostrophic winds are required to produce forecasts more accurate than model climatology.

4. The model takes about two years to spin-up entirely, but velocities differ very little from the equilibrium cycle after just one month.

APPENDIX

Producing The Forcing

The derivation of wind forcing for the model from the operational archive can be broken down into over ten separate stages, each logically separate from the others. It would, however have been rather wasteful to read in and then write out several hundred fields with only one operation performed in between, and so only five jobs were used. These are held in the library MS13.CSLIB.SQHBWIND and are described below. Files beginning with 'F@' are fortran code, and the corresponding 'C@' files are the JCL required to run the fortran. The D@ file is control information. Unless otherwise specified, namelists are read in on fortran unit 5.

C@EXTR

Extracts the relevant data from the operational WGDOS archive into pp format fields. Each month's data spans four or five tapes, so nearly sixty tapes would have had to be accessed at least three times each (more if something went wrong during extraction) to produce the forcing. For efficiency, it was decided to copy this data onto a couple of cartridges. Archived tapes were found to be somewhat unreliable; several backups had to be retrieved from storage in order to rewrite the originals.

FT21 out: restored data (pp-format),

FT81 in: archived data (fields files).

D@EXTR

Namelist information for the extraction program; described more fully in the Operational Numerical Weather Prediction Scheme documentation paper 9.4, and Xappended in the WGDOS documentation, version 3, January 1993.

F@DYMN

The WGDOS archive contains (with some exceptions) four values for each field per

day; the code incorporates noted exceptions and creates daily mean values as required by the model. The days when less than four fields were available were found iteratively: the program DYMN was run, assuming four fields per day unless told otherwise; if the program failed then the last date and the corresponding number of fields read were noted and incorporated into the code, which was then re-run; this continued until a complete set of fields was created.

Data were converted from a 366 to a 360 day year by removing pre-specified days.

Pmsl and 1000mb winds created from either the daily means or the original data were found to be far too strong near mountainous coasts, due to the inaccuracy of the NWP extrapolation algorithms. Each pp-field is therefore multiplied by the NWP land sea mask; this produces missing data where the spurious values would have been, and can be filled in smoothly at a later stage.

C@DYMN

The namelist allows specification of the first and last month to be examined (IMON1 and IMON2), and the code (IPFC) and level (RPLV) of the fields to be processed.

FT09 in: global land-sea mask (pp-format), with a missing data indicator (rmdi) over land,

FT10 in: four times daily raw data for a 366 day year (pp-format),

FT11 out: daily means, 360 day year, with rmdi over land (pp-format).

F@GWND

Produces daily mean westerly and southerly geostrophic wind components and leaves missing data within 40 degrees of the equator. These fields alternate in the output. Calculation of the geostrophic wind from pmsl requires knowledge of the vertical and horizontal density structure, which should be derived from the temperature and humidity fields. To save time and resources, the program reads in a constant density as part of a namelist, this is used for all pmsl calculations. In these experiments a density of 1.38 kg/m^3 was used, which corresponds to dry air at -20° C and 1000mb.

C@GWND

The namelist specifies air density (RHO), if necessary, and the first and last

month to be worked upon (IMON1 and IMON2).

FT10 in: output from C@DYMN,

FT11 out: alternating daily westerly and southerly velocity fields with rmdi over land (pp-format).

F@GRID

Transfers each pp-field to a limited area lat./long. grid with the same spacing, which lies entirely above 40 degrees north, and fills in the missing data. The alternative, just filling in the missing data is computationally too expensive as it involves performing calculations for each grid square in the large band between 40N and 40S left by F@GWND.

F@GRID then interpolates each filled in pp-field to a polar stereographic grid. The polar stereographic grid was chosen by trial and error as the one that most closely fits the square grid (velocity) land mask supplied with the model.

C@GRID

The two namelists contain the grid descriptors for the above-mentioned polar-stereographic and limited area grids. Variables are named like their pp counterparts, but with I or J replacing LB, and Y or Z replacing R.

FT05 in: polar stereographic grid descriptor namelist,

FT09 in: limited area lat./long. grid descriptor namelist,

FT10 in: a 360 day year's worth of output from C@GWND,

FT11 out: a year's worth of filled in polar stereographic alternating westerly and southerly velocity fields (pp-format).

F@PPHB

Converts each velocity pair of polar-stereographic pp-fields to a pair of headerless velocity fields on the square grid, suitable for forcing the model. For simplicity, corresponding polar-stereographic and square grid cells are assumed to overlap exactly. Winds are rotated within the program to change each westerly/southerly pair to an x/y pair of components. The North Pole is filled in by taking the mean of the surrounding winds.

C@PPHB

FT10 in: output from C@GRID,

FT11 out: wind forcing file for the Hibler ice model.

The library contains two further files, used to check PPHB:

F@HBPP

Converts x/y model wind forcing to pp-fields. Uses code added to thheoriginal ice model by J. Thomson (personal comm.) to perform the same conversion for model ice velocities.

C@HBPP

FT10 in: output from C@PPHB,

FT11 out: the first pair of winds from the input, converted to x/y on a polar stereographic grid (pp-format).

Bibliography

Hibler W.D. III (1979): "A dynamic thermodynamic sea ice model.", J. Phys. Oceanogr., **9**, 815-846.

Hibler W.D. III (1980): "Modelling a variable thickness sea ice cover.", Mon. Wea. Rev., **108**, 1943-1973.

Hibler W.D. III and Bryan K. (1987): "A diagnostic ice-ocean model.", J. Phys. Oceanogr., **17**, 987-1015.

Hibler W.D. III and Walsh J.E. (1982): "On modelling seasonal and interannual fluctuations of arctic sea ice.", J. Phys. Oceanogr., **12**, 1514-1523.

Preller R.H. and Posey P.G. (1989): "The Polar Ice Prediction System - a sea ice forecasting system.", Rep. 212, Nav. Ocean Res. and Dev. Act., Stennis Space Centre, Miss. .

Riedlinger S.H. and Preller R.H. (1991): "The development of a coupled ice-ocean model for forecasting ice conditions in the arctic.", J. Geophys. Res., 96 (C9), 16955-16977.

Walsh J.E., Hibler W.D. III, and Ross B. (1985): "Numerical simulation of northern hemisphere sea ice variability, 1951-1980.", J. Geophys. Res., **90** (C3), 4847-4865.

Weather Logs for April (1982-1993): contained in Weather (June, 1982-1993), 37-48 (6).

FIGURES

Figure 1; annual mean winds derived from

(a) 1000mb height.

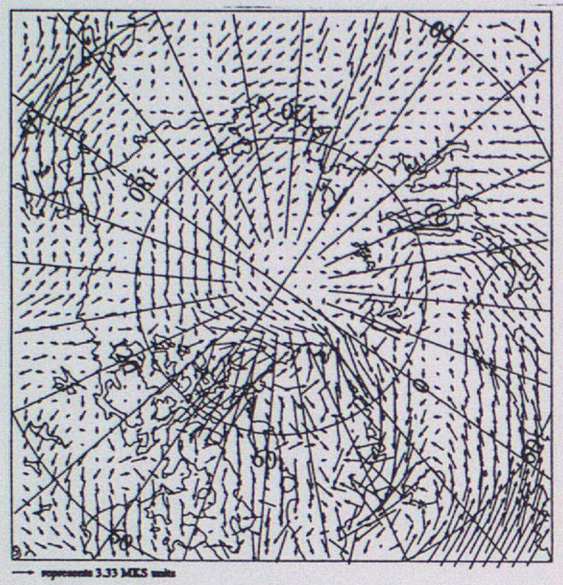

(b) 850mb height

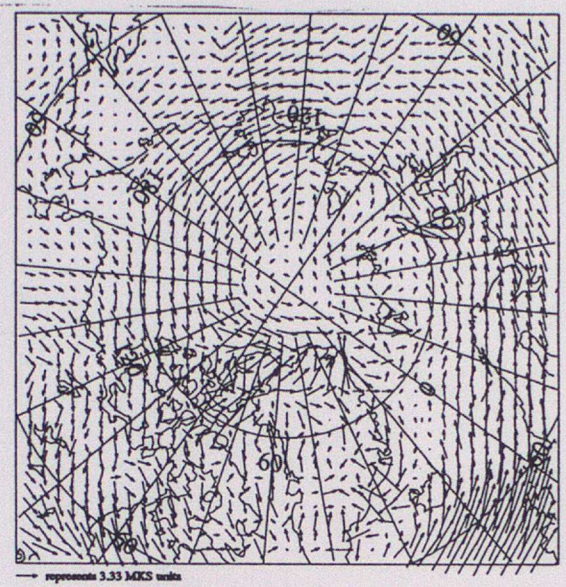

(c) pmsl.

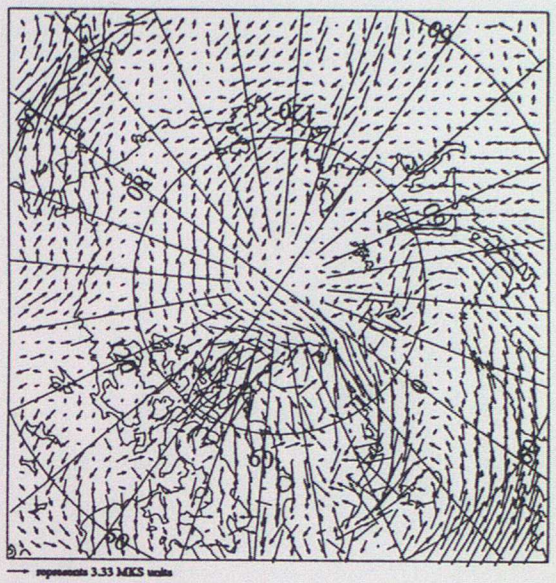

Figure 2; annual mean model ice velocities (year 3) when driven by winds from

(a) 1000mb height

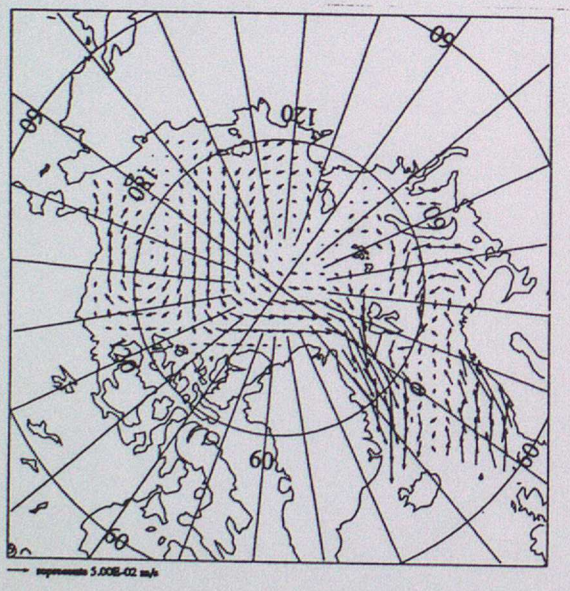

(b) 850mb height

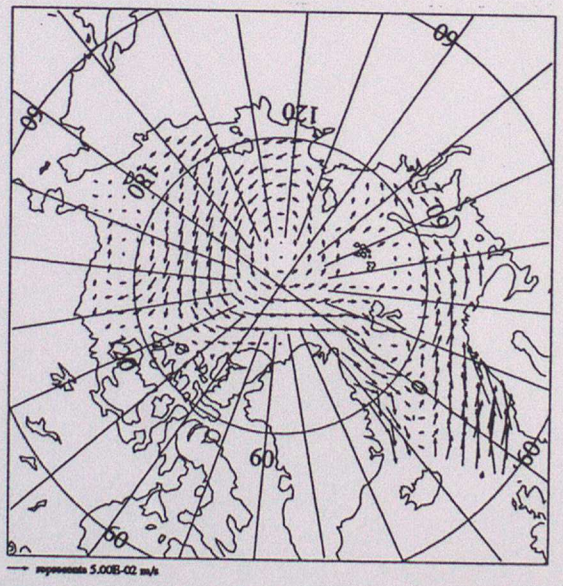

(c) pmsl.

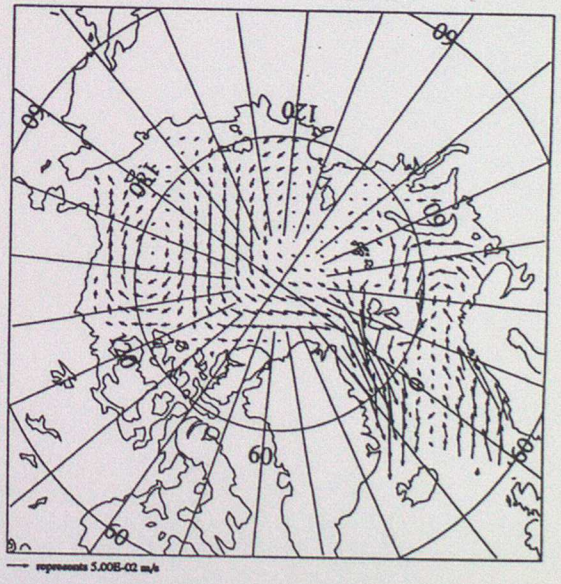

Figure 3; monthly mean model ice velocities (year 3) when driven by winds from 1000mb height for

(a) January (b) April (c) July (d) October

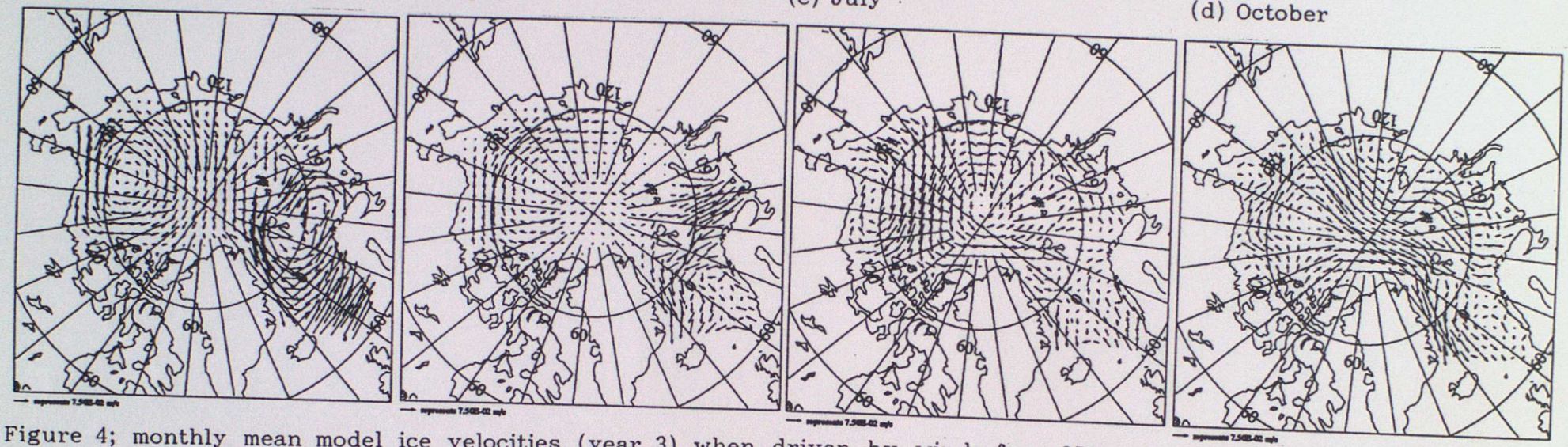

Figure 4; monthly mean model ice velocities (year 3) when driven by winds from 850mb height for

(a) January (b) April (c) July (d) October

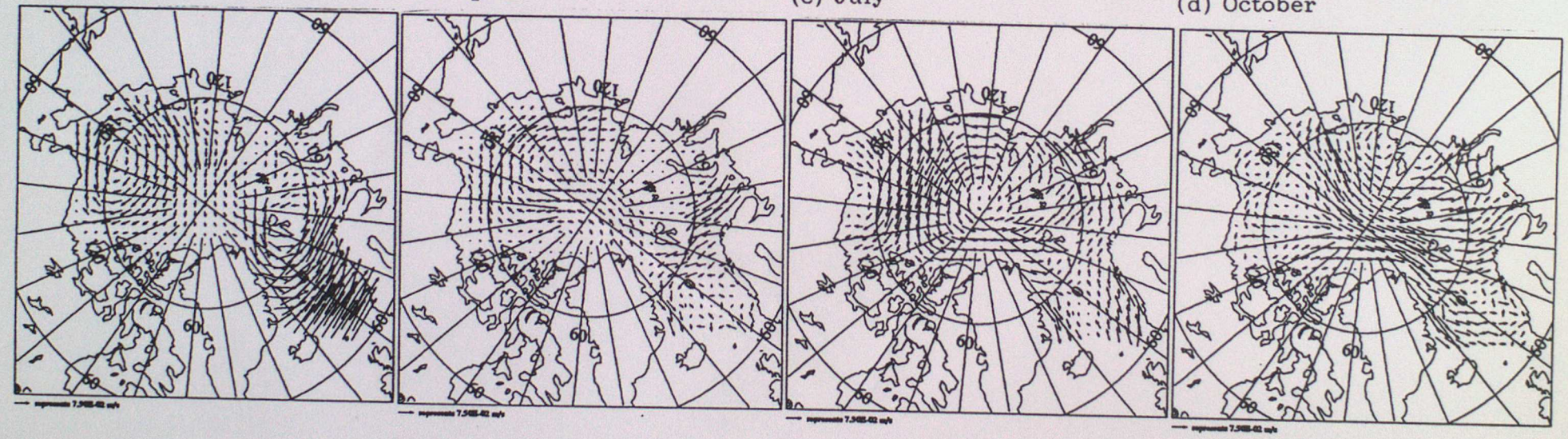

Figure 5; monthly mean model ice velocities (year 3) when driven by winds from pmsl for

(a) January (b) April (c) July (d) October

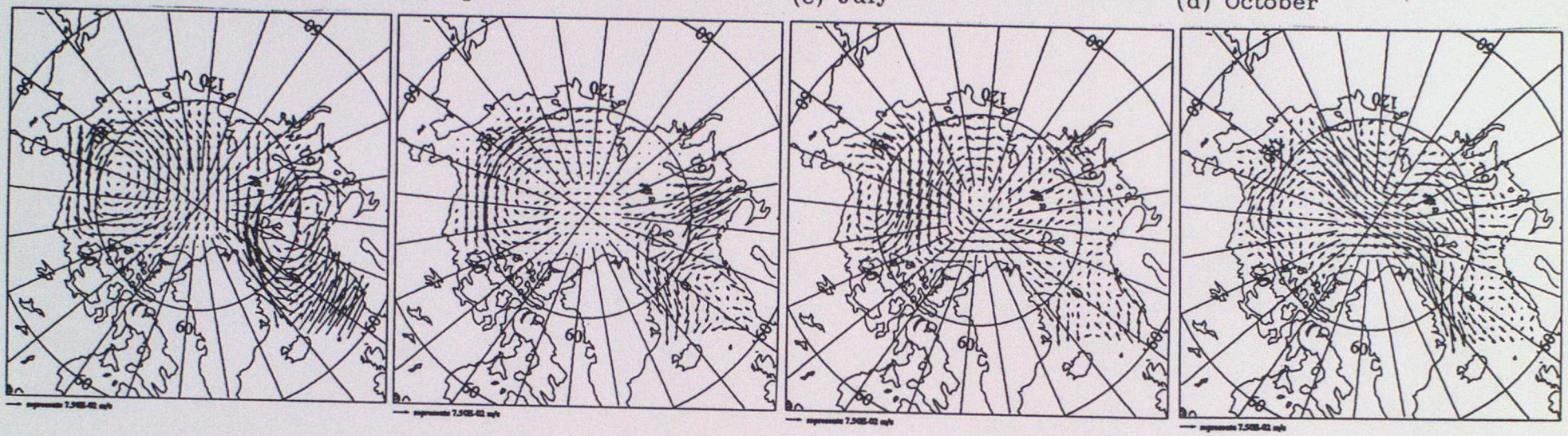

Figure 6; instantaneous model ice depth (year 3) when driven by winds from 1000mb height for the end of

(a) January

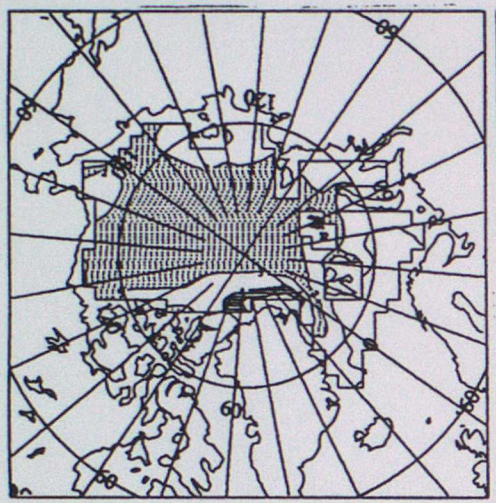

(b) April

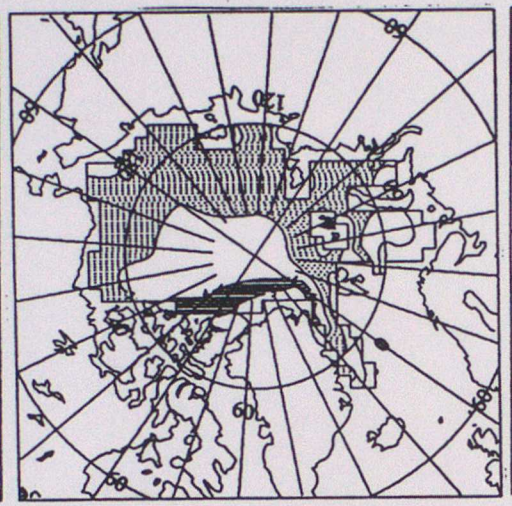

(c) July

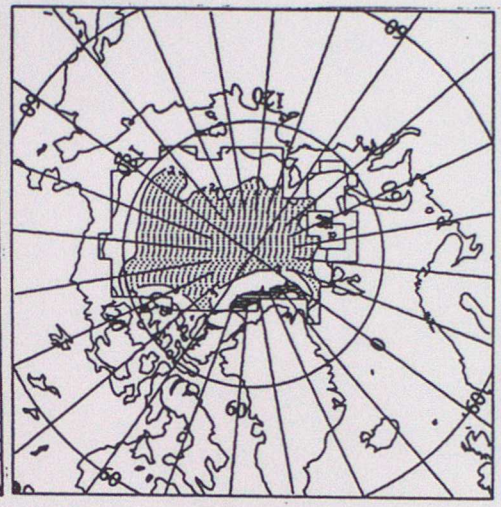

(d) October

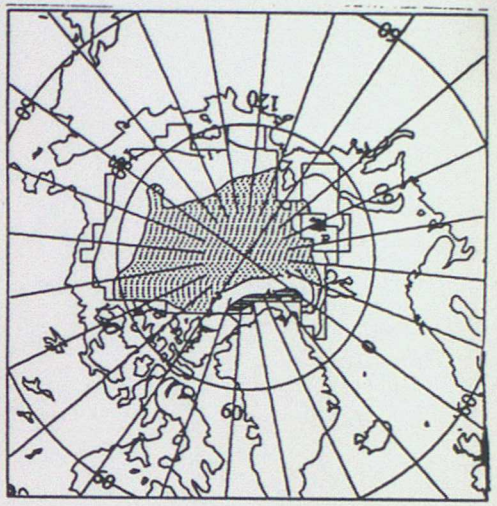

(e) February

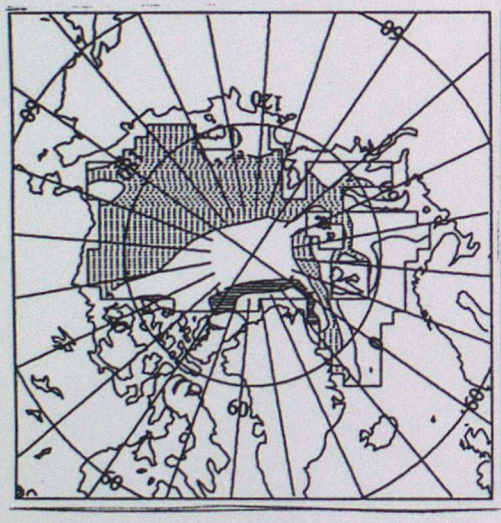

(f) August

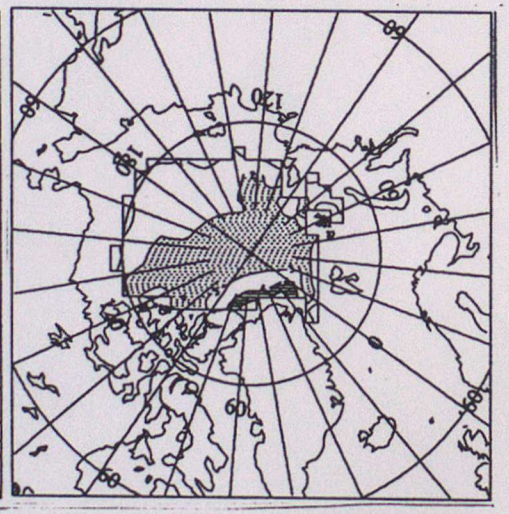

Figure 7; instantaneous model ice depth (year 3) when driven by winds from 850mb height for the end of
(a) January (b) April (c) July (d) October

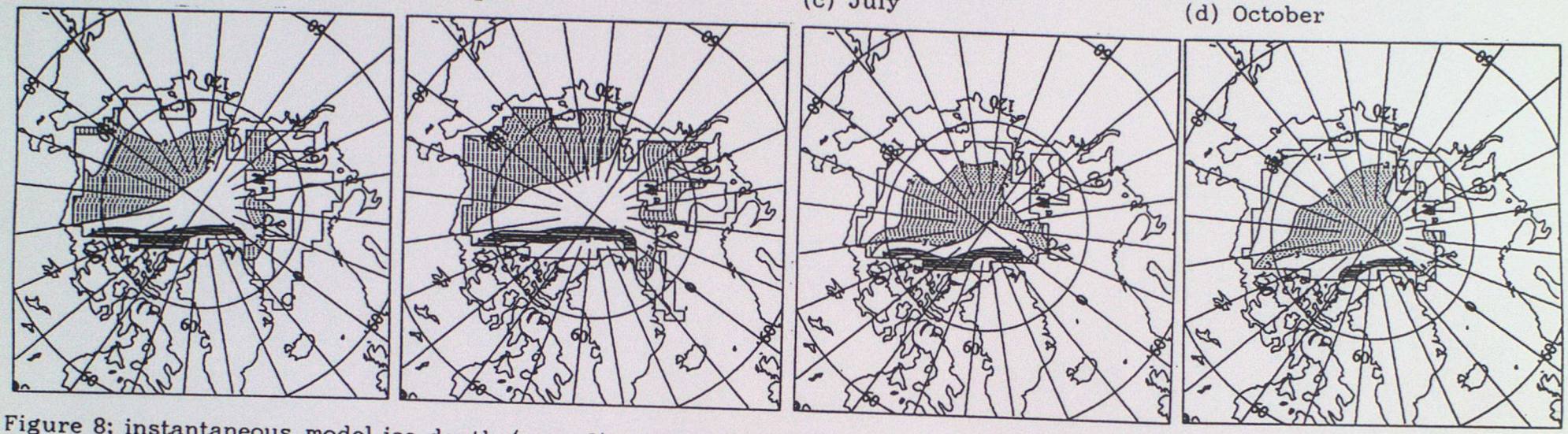

Figure 8; instantaneous model ice depth (year 3) when driven by winds from pmsl for the end of
(a) January (b) April (c) July (d) October

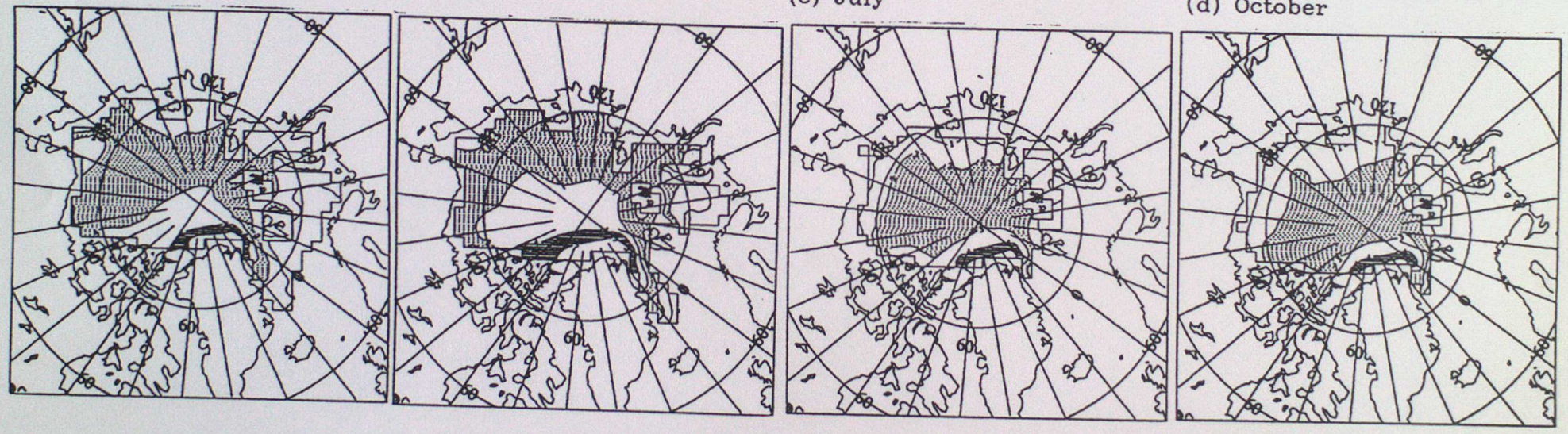

Figure 9; ice extent derived from the JIC ice edge bulletins of 1992 for

(a) January 17th (b) April 10th (c) June 12th (d) October 16th

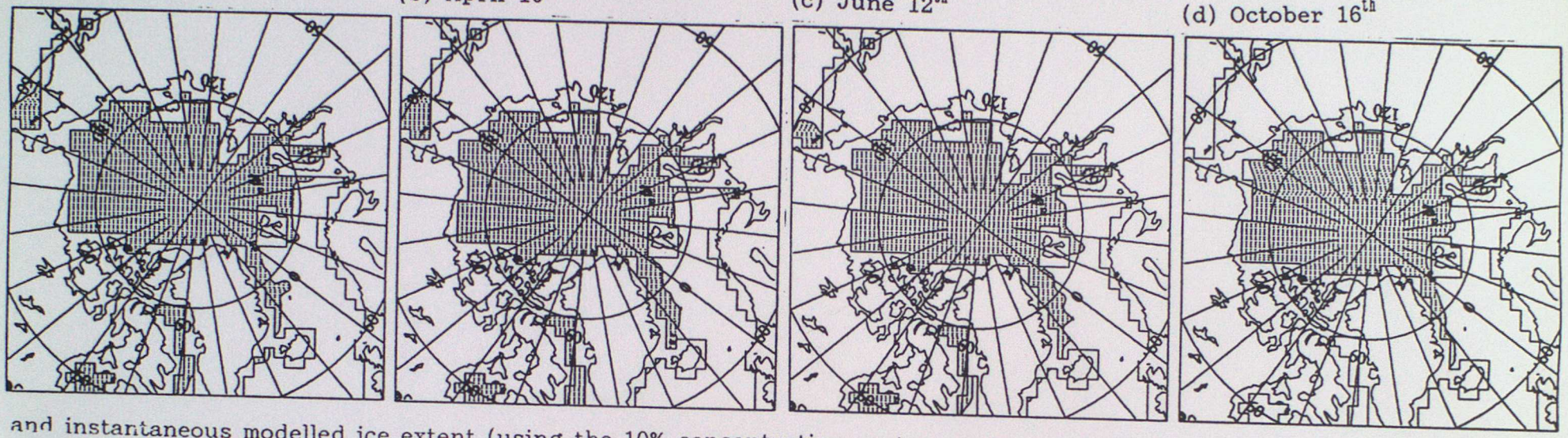

and instantaneous modelled ice extent (using the 10% concentration contour as the ice edge) (year 3) when driven by winds from 1000mb height for the end of

(e) January (f) April (g) June (h) October

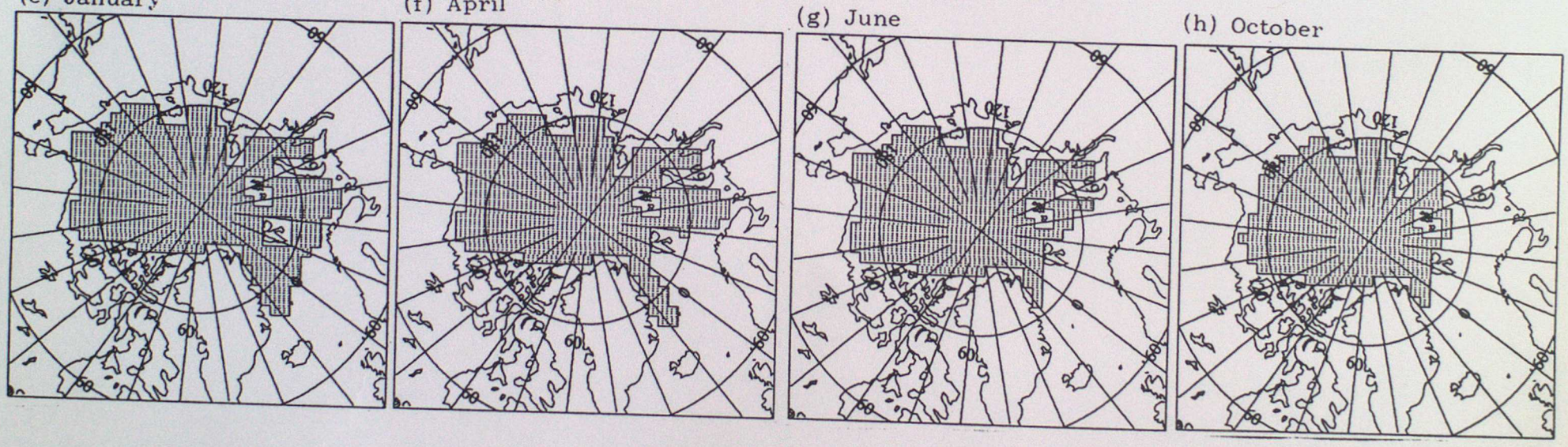

Figure 10; from Walsh et al. (1985)

mean ice thickness

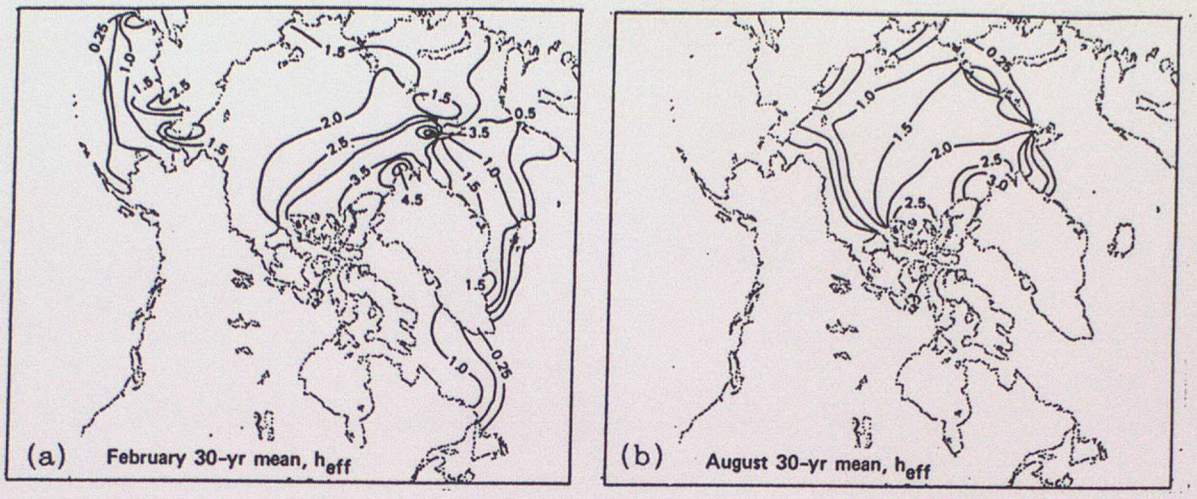

mean ice thickness

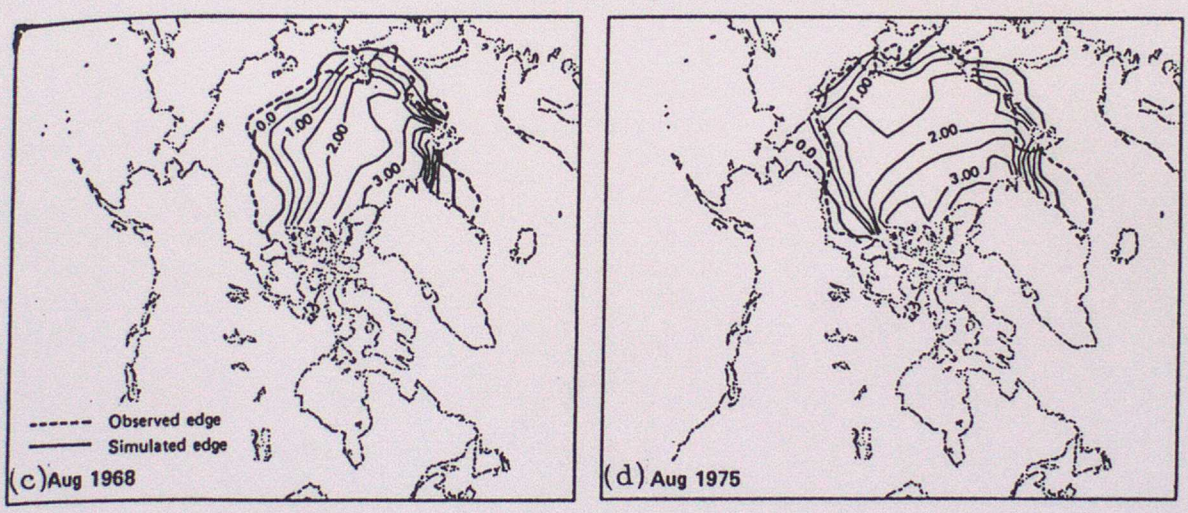

mean ice velocity (vectors are scaled to correspond to 25% of the annual displacements in regions of year round ice cover)

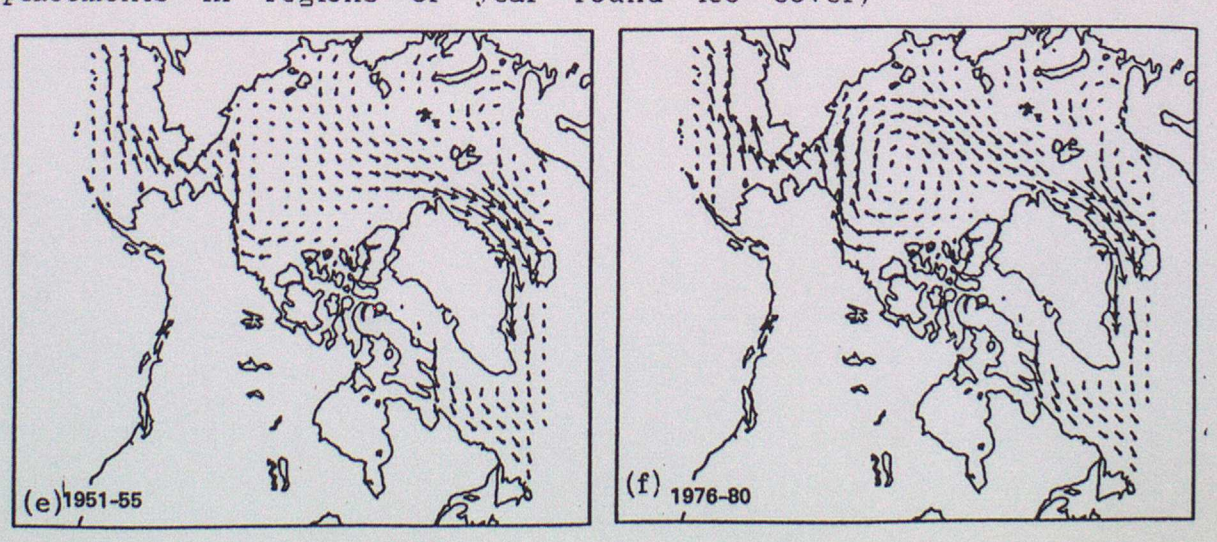

Figure 11; instantaneous model ice depth when driven by winds from 1000mb heights (1992) for the end of

(a) January (year 1)

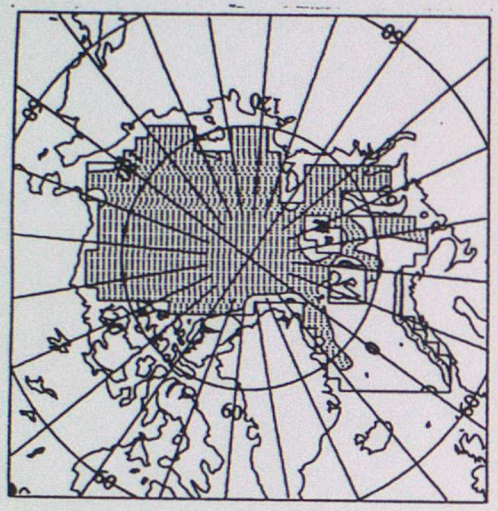

(b) April (year 1)

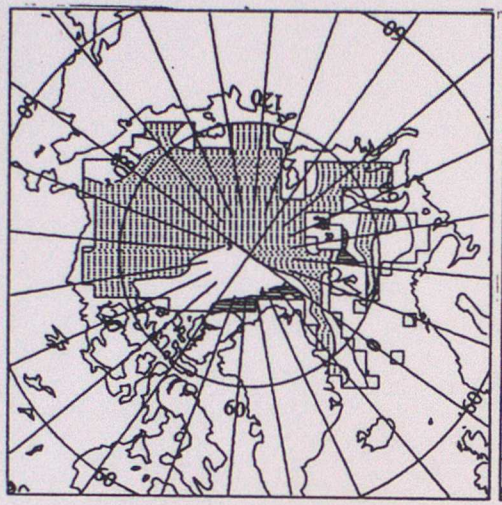

(c) July (year 1)

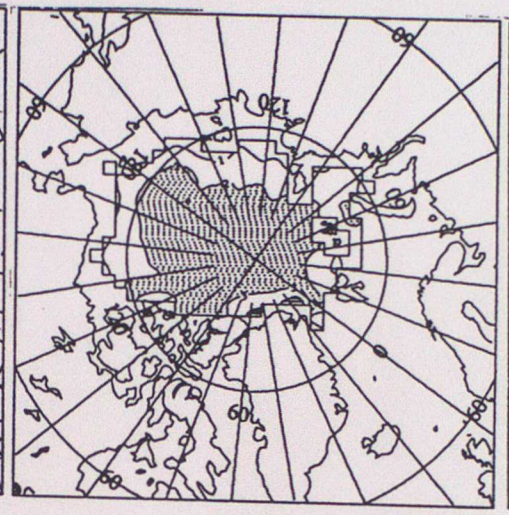

(d) October (year 1)

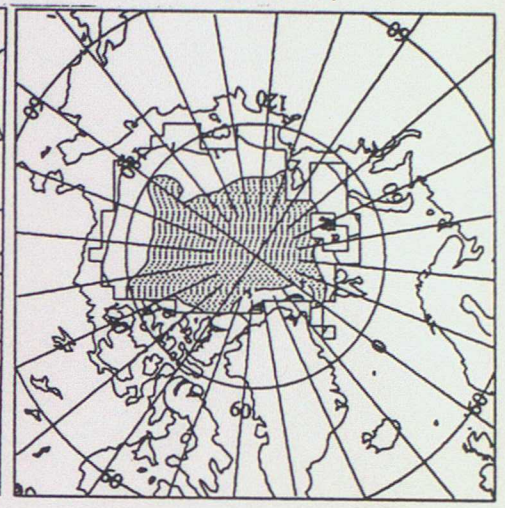

(e) January (year 2)

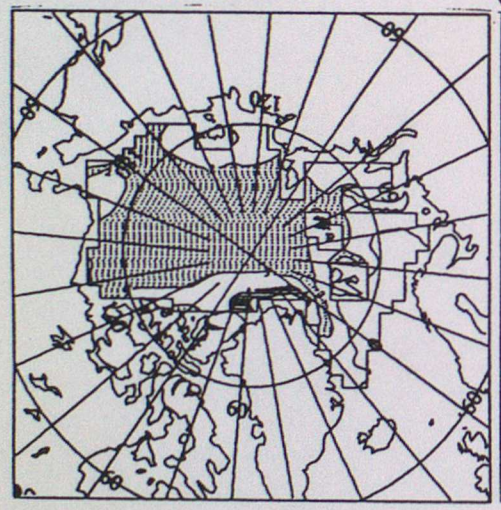

(f) April (year 2)

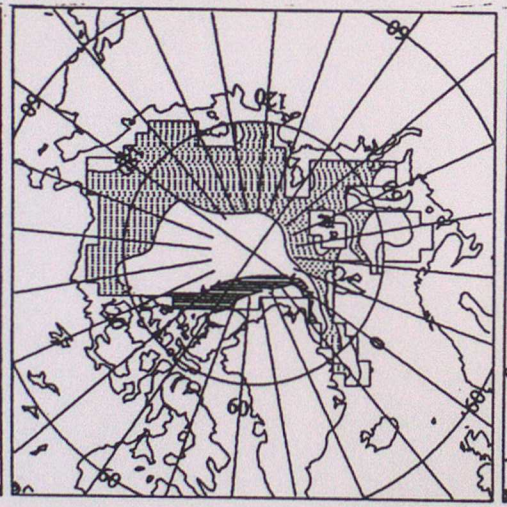

(g) July (year 2)

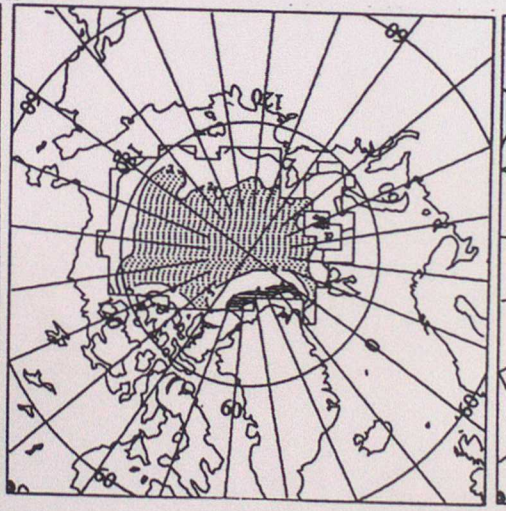

(h) October (year 2)

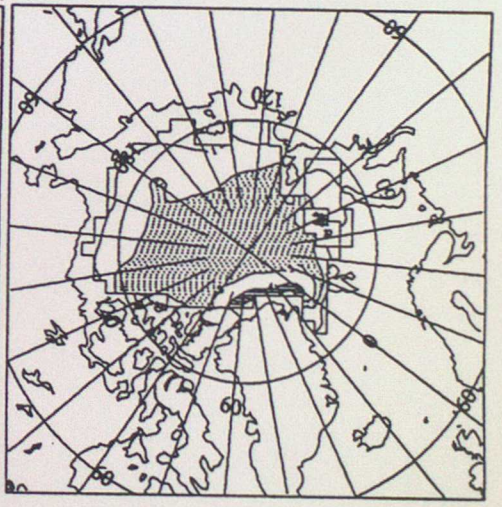

Figure 12; monthly mean model ice velocity when driven by winds from 1000mb heights (1992)

(a) January (year 1)

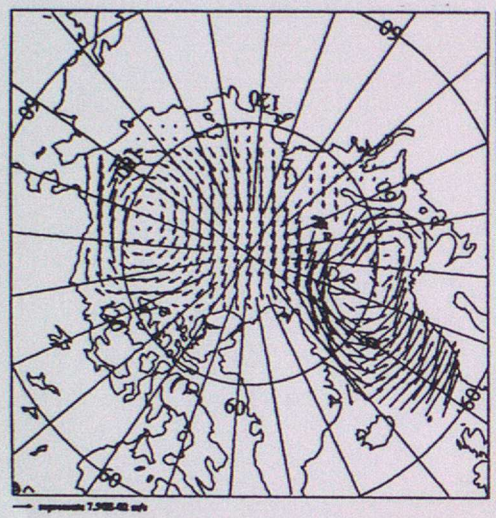

(b) April (year 1)

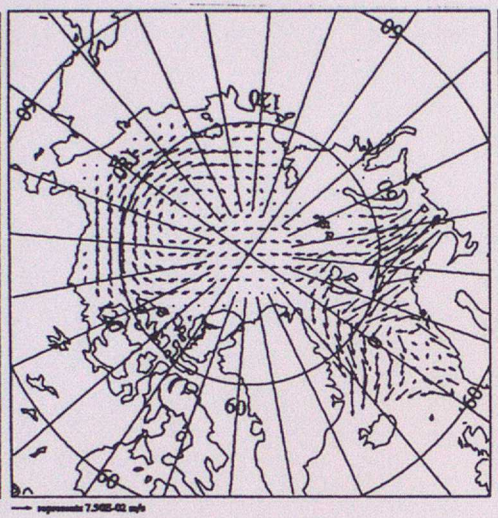

(c) July (year 1)

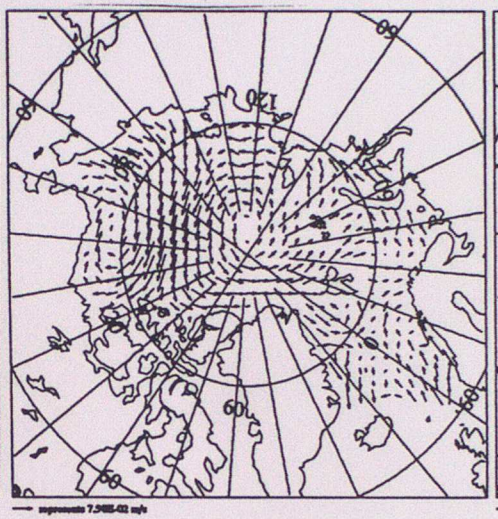

(d) October (year 1)

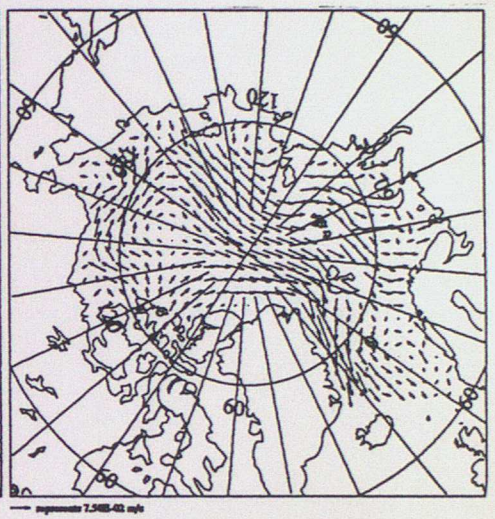

(e) January (year 2)

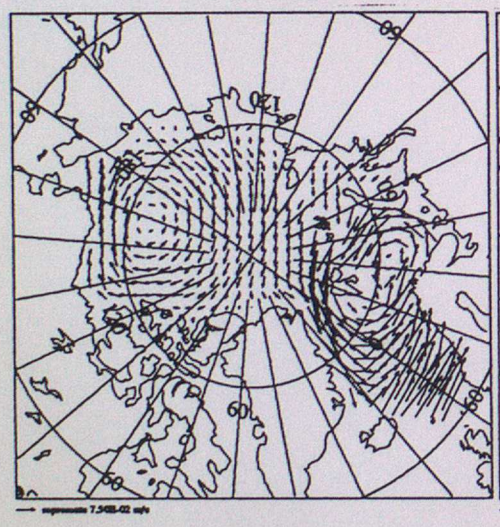

(f) April (year 2)

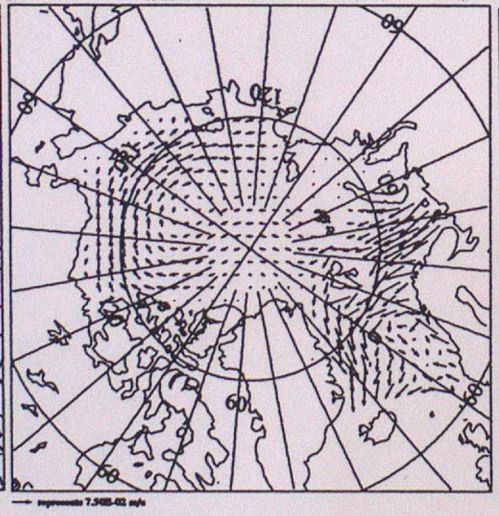

(g) July (year 2)

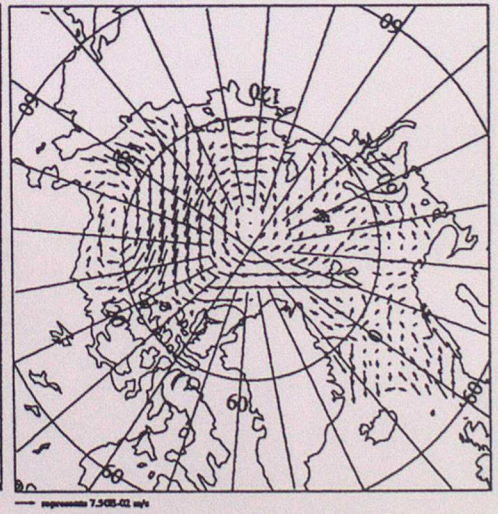
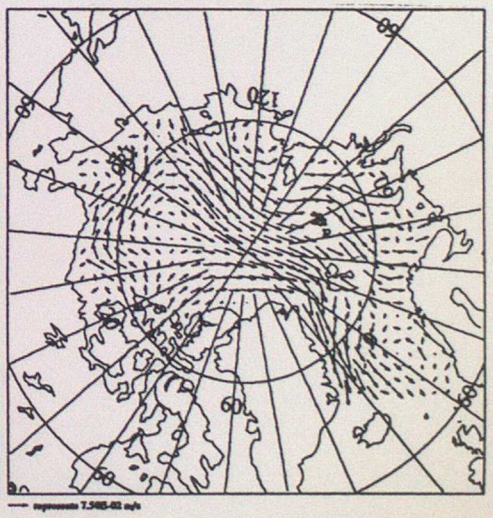
(h) October (year 2)